

Aggregates in Ionic Liquids and Applications Thereof

J. D. Marty and N. Lauth de Viguerie
University of Toulouse
France

1. Introduction

Due to the increasing consciousness of environmental problems, chemical processes were developed with their environmental burden in mind. This results in the past decade, to the definition of Green chemistry encouraging the design of products and processes that reduce or eliminate the use and generation of hazardous substances. Moreover regulation (EC) No 1907/2006 of the European Parliament and of the Council of 18 December 2006 concerning the Registration, Evaluation, Authorisation and Restriction of Chemicals (REACH), gives greater responsibility to industry to manage the risks from chemicals and to provide safety information on the substances. REACH Regulation also calls for the progressive substitution of the most dangerous chemicals when suitable alternatives have been identified. Hence, from both societal and legislative point of views, there is a great need to find viable replacements for volatile organic compounds (VOC) used in usual chemical process. Of special interest is the case of solvents. They are used in most areas including synthetic chemistry, analytical chemistry, pharmaceutical production and processing, product purification, extraction and separation technologies, and also in the modification of materials. Due to the hazards of many conventional solvents (e.g. toxicity and flammability), knowledge of alternative, greener solvents is compulsory. The most useful alternatives to traditional solvents are supercritical CO₂ (where the gas is compressed until it is nearly as dense as a liquid), ionic liquids and water.

Room temperature ionic liquids (RTILs) are of special interest with unique applications as tunable and environmentally benign solvents with negligible vapor pressures, high chemical and thermal stability, high fire resistance and wide liquid temperature range and electrochemical windows. Moreover, owing to their molecular structure associating a cation and an anion, their physicochemical properties can be easily modulated by changing one of the ions. Hence, ionic liquids are now widely used in organic synthesis and chemical separations due to their high solvation ability and their tunable nature. (Dupont et al., 2002; Ranke et al., 2007) Lastly, corresponding to structured polar medium, RTILs can be also exploited to investigate molecular aggregation. Some authors have described in the past few years the ability of ILs to form various aggregates such as micelles, (Patrascu et al., 2006; Gayet et al., 2010b) vesicles, (Kimizuka and Nakashima, 2001; Nakashima and Kimizuka, 2002; Hao et al., 2005; Gayet et al., 2010a) non aqueous microemulsions (Gao et al., 2004; Eastoe et al., 2005; Gayet et al., 2009) or lyotropic phases (Evans et al., 1983; Wang et al., 2004; Araos and Warr, 2005). This gives access to new applications in green chemistry and

opens new research directions towards micellar catalysis in IL media, solvation enhancement for apolar entities, biocatalysis, nanomaterials synthesis, etc. (Hao and Zemb, 2007; Greaves and Drummond, 2008) The organized phases in ionic liquids make it possible to consider a new control of the reactivity including the properties of ILs and of organized media. Thus, the replacement of water by ILs for which the physicochemical structure and properties can be customised, should make it possible to widen the choice of the reactions considerably. Here we will describe some examples of each class of materials and will try to compare the results obtained to those given in water or structured solvents.

2. Methodology.

In this section, the main physical-chemistry methods involved in the characterization of aggregates in ILs were described.

2.1 Materials

Alkyl poly-(oxyethyleneglycol) ethers (purity \geq 98 %), 1,2-dipalmitoyl-*sn*-glycero-3-phosphocholine (DPPC) and anhydrous toluene were purchased from Sigma-Aldrich and were used as received. Triton® X-100 (TX-100) from Sigma-Aldrich was dried at 60°C under vacuum for 3 hours and filtered under nitrogen through PTFE (0.45 μ m) prior to use. Ionic liquids, 1-butyl-3-methylimidazolium tetrafluoroborate (bmimBF₄), 1-butyl-3-methylimidazolium hexafluorophosphate (bmimPF₆), 1-butyl-3-methylimidazolium bis(trifluoromethylsulfonyl)imide (BmimNTf₂), 1-ethyl-3-methylimidazolium bis(trifluoromethylsulfonyl)imide (emimNTf₂) were purchased from Solvionic (www.solvionic.com; purity \geq 98 %) and were dried under low pressure around 70°C before use. N-benzylpyridinium bis(trifluoromethylsulfonyl)imide (bnPyNTf₂) was synthesized as previously described (Patrascu et al., 2004).

2.2 Micelles in ILs

The viscosity of the ionic liquids was measured with an AR 1000 rheometer (from TA) equipped with a temperature controller and a cone/plate geometry (diameter=40 mm, angle=2 deg). Zero-shear viscosities were extrapolated from the steady state shear viscosities curves obtained at 25 °C. Surface tension experiments were performed using the pending-drop technique (KRÜSS instrument, model DSA10-Mk2). The C_nE_m/bmimX solutions were prepared by dissolving a precise weight of surfactant [using a Sartorius microbalance Genius model (\pm 0.05 mg)] in a defined volume of ionic liquid [measured by a Finnpiptette PDP from Labsystem (\pm 0.1 μ l) and a Repeater Plus Pipette, model 4980 from Eppendorf (\pm 2 μ l)]. The solutions were stirred and held at 60 °C for 2 h and then cooled to 25 °C before use.

Light scattering measurements of micelles were performed on a homemade instrument based on a 647.1 nm ionized krypton laser source (Innova 90 model from Coherent, vertically polarized beam), focalized on the sample by a lens corrected for spherical aberrations (focal length 100 mm). A EMI 9863 photomultiplier with a 200 μ m slit detector mounted on a BI200-SM goniometric arm from Brookhaven Instruments was used as detector. The amplified signal was treated by a BI9 K digital correlator from Brookhaven Instruments. The samples were filtered (0.45 μ m hydrophobic Teflon filters for the BmimPF₆ solutions and on 0.45 μ m hydrophilic cellulose acetate Sartorius filters for the BmimBF₄ solutions). The scattering cells were previously rinsed with filtered ionic liquids. The following viscosity values were used: 78 cP for bmimBF₄ and 250 cP for bmimPF₆.

2.3 Vesicles in ILs

Preparation of lipid vesicles. A stock solution of DPPC (2.10^{-2} mol.L $^{-1}$) in chloroform/methanol (9:1, v/v) was prepared and stored at 4°C. 400 μ L of these lipid solutions were placed in a vial and solvent were evaporated under a nitrogen stream. Residues were desiccated under vacuum for 2 h (1 Torr). The dried lipid samples were hydrated in 200 μ L of pure IL or IL/water mixtures and heated to 80°C for 20 min (this temperature is higher than the gel-to-liquid transition temperature (T_m)). The sample was immediately vortexed for 4 min. The vesicle solutions ([DPPC]= 4.10^{-2} mol.L $^{-1}$ i.e. 2.93% w/v) so prepared were then stored at 4°C overnight.

Differential Scanning Calorimetry (DSC). Thermal transitions in vesicles were measured on a Perkin-Elmer PYRIS1 calorimeter, using heating and cooling rates from 2 to 20°C/min. A 25 μ L quantity of each vesicular solution was loaded in pans and allowed to equilibrate at initial temperature for 20 minutes. Data were collected at different rates from 1 to 20°C between 0 and 120°C. Main transition temperature was determined as the peak maximum of an endothermic transition extrapolated to 0°C/min. Lipid concentration in ionic liquids was fixed at $4.2.10^{-2}$ mol.L $^{-1}$.

Transmission electronic microscopy (TEM). TEM measurements were made on a Jeol JEM - 2100 Transmission Electron Microscope operated at an accelerating voltage of 100 kV in the Institut Fédératif d'Exploration Fonctionnelle des Génomes (Toulouse, France). Samples were negatively stained by a solution of sodium phosphotungstate.

Small Angle Neutron Scattering (SANS). SANS experiments were performed with the PACE spectrometer at the Orphée reactor (LLB, Saclay). DPPC-IL and DPPC-IL-water mixture were put inside quartz cells of 1 or 2mm gap and measured at 20° ([DPPC] = 1 %w/v). Three spectrometer configurations were used: a neutron wavelength (λ) of 7Å with a sample to detector distance of 3m, then another distance of 1m and a wavelength of 17Å with a distance of 4.8m. The scattering vector range thus reached was $0.0025 < q$ (Å $^{-1}$) < 0.35 . Scattering intensities have also been normalized by the incoherent signal delivered by a 1 mm gap water sample in order to account for efficiency of detector cells. Absolute values of the scattering intensity, $I(q)$ in cm $^{-1}$, were obtained from the direct determination of the number of neutrons in the incident beam and the detector cell solid angle. No background has been subtracted to the copolymer sample scattering, thus a flat incoherent signal has been observed at high q values.

2.4 Non-aqueous microemulsions

Phase diagram determination. Each component (anhydrous toluene, Triton® X-100 and bnPyrNTf $_2$) was added by weight under inert atmosphere on a Sartorius balance with a precision of ± 0.01 mg. The mixtures were stirred until clear and homogeneous at 27°C. The phase diagram was built by titration with TX-100 as follows: required weight of toluene and bnPyrNTf $_2$ were initially mixed, then TX-100 was added until transition from turbidity to transparency.

Electrical conductivity experiments. Conductivity measurements were performed on a Mettler Toledo SevenMulti conductimeter using an InLab730 probe with a platinum electrode of cell constant of 0.563 cm $^{-1}$. In the experiments, the sample and the electrode were sealed in a glass cell, which was placed in a water bath at $27.0 \pm 0.1^\circ\text{C}$. Fractionated volumes of toluene (100 μ L) were successively added to the microemulsion using a Hamilton syringe.

Dynamic Light Scattering measurements (DLS). DLS Measurements were carried out at $27.0^\circ\text{C} \pm 0.1^\circ\text{C}$ with a Malvern Instrument Nano-ZS equipped with a He-Ne laser ($\lambda = 633$ nm). Samples were introduced into Helma cells (111-OS 10 mm) through 0.45 μ m PTFE micro-

filters prior to measurements. The correlation function was analyzed via the general purpose method to obtain the distribution of diffusion coefficients (D) of the solutes, and then the apparent equivalent hydrodynamic radius (R_h) was determined using the Stokes-Einstein equation.

Small Angle Neutron Scattering. SANS experiments were performed with the PAXY spectrometer at the Orphée reactor (Laboratoire Léon Brillouin, Saclay). Microemulsion solutions were put inside Hellma quartz cells of 1 or 2mm gap. Temperature was maintained constant at $27 \pm 0.2^\circ\text{C}$. Two spectrometer configurations were used: a neutron wavelength (λ) of 4\AA with a sample to detector distance of 1.435 m and a wavelength of 10\AA with a distance of 2.035m. The neutron wavelength distribution $\Delta\lambda/\lambda$ is 0.11 (FWHM). The incident collimation was obtained from two circular holes 2.5 m apart, one with a diameter of 22 mm and the second, close to the sample, with a diameter of 7.6 mm. The scattering vector range thus reached was $0.01 < q (\text{\AA}^{-1}) < 0.4$. The efficiency of the detector cells was normalized by the incoherent signal delivered by 1 mm gap water cell. Absolute values of the scattering intensity, $I(q)$ in cm^{-1} , were obtained from the direct determination of the number of neutrons in the incident beam and the detector cell solid angle. Several series of blank samples (mixtures of H and D toluene) were also measured to plot precise calibration curves to subtract from each IL solution.

3. Micelles in room temperature ionic liquids

The micellar aggregation behavior of surfactants in ILs has been investigated in recent years. Evans and co-workers first reported the aggregation behavior of alkyltrimethylammonium bromides, alkylpyridiniums bromides and Triton X-100 in ethyl ammonium nitrate (Evans et al., 1982; Evans et al., 1983). More recently, premicellar aggregation in 1-butyl-3-methylimidazolium chloride and hexafluorophosphate was detected using inverse gas chromatography (Anderson et al., 2003). Merrigan et al. have demonstrated that imidazolium cations with long fluorinated tails act as surfactants and appear to self-aggregate within imidazolium-based ILs (Merrigan et al., 2000). The possible aggregate formation by nonionic surfactants Brij-35, Brij-700, Tween-20, and Triton X-100 in emimNTf₂ was observed on the basis of the response of solvatochromic probes (Fletcher and Pandey, 2004). Tran and Yu have reported that nonionic surfactants N-dodecylsultaine and caprylyl sulfobetaine formed micelles in bmimPF₆ and emimNTf₂ (Tran and Yu, 2005). Moreover, nonionic surfactant self-assembly into micelles in ethylammonium nitrate was examined (Araos and Warr, 2008).

The ability of a series of pure alkyl poly-(oxyethyleneglycol) ethers in 1-butyl-3-methylimidazolium (bmim) ILs with various counter ions [BF₄⁻, PF₆⁻ and Tf₂N⁻, that is, bis(trifluoromethylsulfonyl)amide; Figure 1] to form micellar systems was investigated.

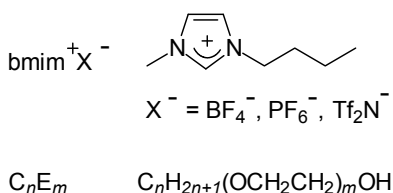


Fig. 1. Molecular structures of the ILs and surfactants used herein ($n=12-16$; $m=4-8$).

Nonionic surfactants, denoted C_nE_m ($n=12-16$; $m=4-8$), were chosen to avoid the exchange of counter ions with the solvent. The formation of micelles was clearly evidenced using surface tension, multi-angle dynamic light scattering (DLS) and small-angle neutron scattering (SANS) measurements (Patrascu et al., 2006).

3.1 Surface tension measurements.

Surface tension measurements were performed to probe the aggregation behavior of the surfactants in bmimBF_4 . For all the selected surfactants, the surface tension of the C_nE_m/bmimBF_4 solutions decreased when the surfactant concentration increased (Figure 2a and 2b). This indicated their adsorption at the air/solution interface. The Szyszkowski-Langmuir adsorption equation (Fainerman et al., 1998) fitted well this decrease, leading to an estimation of the area per surfactant molecule at the air/ bmimBF_4 interface, comparable or lower than the one found at the air/water interface (Table 1). The differences between bmimBF_4 and water may be related to a change in the organization and/or solvation state of the adsorbed surfactants. In bmimBF_4 , like in water, the molecular area of the surfactant decreased with increasing alkyl chain length or decreasing number of oxyethylene groups. This reflects the equilibrium conditions of the self-assembly process.

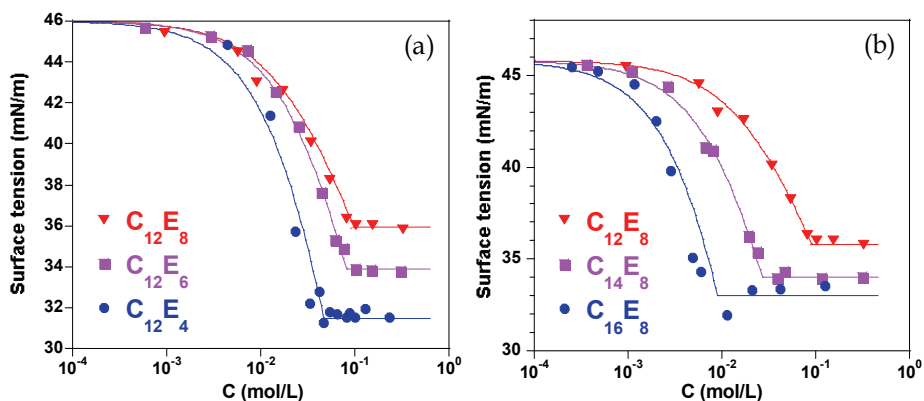


Fig. 2. Surface tension of solutions of C_nE_m ($n=12-16$; $m=4-8$) in bmimBF_4 . a) Effect of hydrophilic ethyleneoxide part ; b) Effect of hydrophobic alkyl chain length

This initial decrease of the surface tension is followed by an abrupt change in the slope of the surface tension versus C (Figures 2a and 2b). After this breaking point, the surface tension of the solutions remains more or less constant. Such behavior suggested the formation of micelles within the ILs, where the break point corresponds to a critical micelle concentration (cmc). The cmc values in ILs were two to four orders of magnitude higher than those in aqueous systems but are equivalent to or slightly higher than those in formamide (Table 1).

The influence of the hydrophilic and hydrophobic moieties on the cmc in each solvent (water, formamide and bmimBF_4) was shown in Figures 3a and 3b respectively. The values of the slope are related to the contribution of hydrophilic and hydrophobic groups on the cmc. In formamide, these contributions are significantly lower than in water and IL.

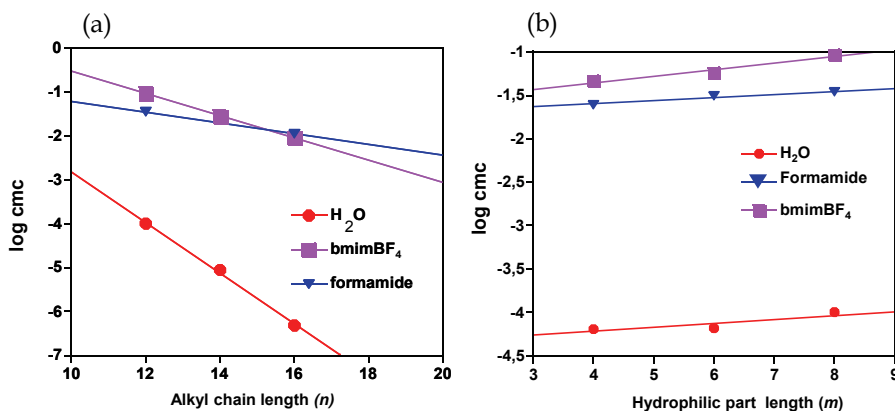


Fig. 3. log cmc versus a) hydrophobic alkyl chain length ($n=12, 14, 16$); b) number of ethyleneoxide groups ($m=4, 6, 8$).

C_nE_m	bmimBF ₄		H ₂ O		Formamide	
	S [Å ²] ^[a]	cmc [mmol L ⁻¹] ^[b]	S [Å ²] ^[c]	cmc [mmol L ⁻¹] ^[d]	S [Å ²] ^[e]	cmc [mmol L ⁻¹] ^[f]
C ₁₆ E ₈	22±2	9±1		0.0005		11
C ₁₄ E ₈	38±3	27±1	49	0.009		
C ₁₂ E ₈	65±2	93±2	66	0.1		35
C ₁₂ E ₆	30±2	57±2	61	0.067	63	31
C ₁₂ E ₄	26±2	46±1	46	0.065		25

Table 1. Cmc and molecular area (S) of C_nE_m in bmimBF₄, water and formamide at 25 °C. [a] Estimated through a fit to the Szyszkowski-Langmuir adsorption equation. [b] Deduced from surface tension measurements. [c] From (Rosen et al., 1982; van Os et al., 1993). [d] From (Berthod et al., 2001). [e] From (Couper et al., 1975). [f] From (McDonald, 1967; Jonstromer et al., 1990), some cmc measurements were performed at 21 °C.

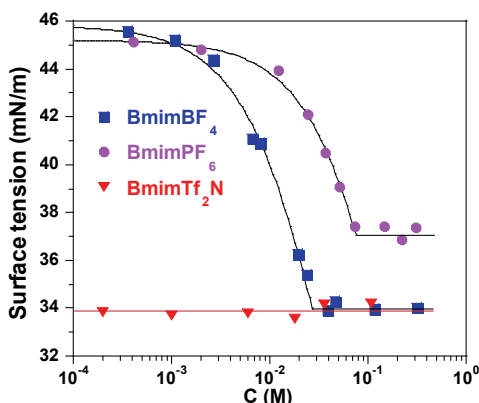


Fig. 4. Surface tension of C₁₄E₈ in bmimBF₄ (■), bmimPF₆ (●) and bmimNTf₂ (▲) at 25 °C.

3.2 Multi-angle dynamic light scattering and small-angle neutron scattering experiments.

To verify the shape and size of aggregates in ILs, multi-angle DLS and SANS measurements were performed and results were summarized in Table 2.

C_nE_m	bmimBF ₄		bmimPF ₆		H ₂ O		formamide	
	r_H [nm] [a]	N_{agg} [b]	r_H [nm] [a]	N_{agg} [b]	r_H [nm] [d]	N_{agg} [e]	r_H [nm] [f]	N_{agg} [g]
C ₁₆ E ₈	3.2±0.4	≈145			≈3.7	10±15	≈4	
C ₁₄ E ₈	2.5±0.3	≈75	1.4±0.1	≈15				
C ₁₂ E ₈	1.6±0.1	≈20			≈3.1	95±5		
C ₁₂ E ₆	2.3±0.1	≈75			≈3.2	140±15	≈2	≈30
C ₁₂ E ₄	- [c]	- [c]				165±62	≈2	

Table 2. Hydrodynamic radius (r_H) and aggregation number (N_{agg}) of C_nE_m micelles in bmimBF₄, water and formamide at 25 °C. [a] Deduced from DLS measurements at 4 cmc and 8 cmc concentrations. [b] See text. [c] At 25 °C and 4 cmc concentration cloud point is already reached. [d] From (Zulauf et al., 1985) [e] From (Herrington and Sahi, 1988);(Zulauf et al., 1985), the data corresponding to the C₁₂E₄ surfactant was obtained near 0 °C. [f] From (Couper et al., 1975; Jonstromer et al., 1990), the data corresponding to the C₁₆E₈ surfactant was obtained at 40 °C. [g] From (Couper et al., 1975).

DLS experiments realized on the C_nE_m /bmimBF₄ solutions showed the presence of spherical objects with sizes between 1.6 and 3.2 nm (Table 2). The hydrodynamic radii in ILs were smaller than those in water and close to those found in formamide. The use of bmimBF₄ did not allow us to achieve SANS due to the neutron absorption by boron atoms. Thus, SANS experiments were performed on bmimBF₆ solutions. For concentrations higher than the cmc, the scattered neutron intensity versus the scattering vector was well-fitted by a general Guinier model. The presence of globular aggregates with a radius of approximately 1.3±0.2 nm was identified for C₁₄E₈/bmimBF₆ system. This value was comparable with the one obtained from DLS measurements.

Using an approximation of the surfactant volumes occupied in the micelle (Zulauf et al., 1985; van Os et al., 1993), we estimated the aggregation number in the micelles. Either increasing the alkyl chain length or decreasing the poly(oxyethylene) chain length contributes to both an enhanced hydrophobicity and an increase in aggregation number. Aggregation numbers in RTILs are smaller than those in water. As in water (Herrington and Sahi, 1988; van Os et al., 1993) micelle size and aggregation number increased with the alkyl chain length or the number of oxyethylene groups.

All these results proved that surfactant aggregation can occur in ILs and that the formed aggregates were micelle-like. The size and aggregation number of the micelles can be tuned by changing the exact nature of the IL.

4. Vesicles

Only few examples of vesicles have been observed in pure ILs. Their formation was first evidenced with a glycolipid L-glutamate derivative in two ether-containing ILs (N,N'-dialkylimidazolium bromides Me-Im-C₂OC₁ and Me-Im-C₁OC₁) by means of differential scanning calorimetry (DSC) and dark-field optical microscopy (Kimizuka and Nakashima,

2001). DSC measurements showed an endothermic peak (T_c) at 40°C and at 51°C in Me-Im- C_2OC_1 and in Me-Im- C_1OC_1 respectively. This indicates that the phase transition characteristics of the glycolayers are affected by the chemical structure of the IL. In addition, a similar behavior was observed for dialkyldimethylammonium bromides in the same ILs (Nakashima and Kimizuka, 2002). In both studies, bilayer vesicles were observed by dark-field optical micrographs only above the transition temperature. Moreover, no aggregate was formed with these surfactants in a conventional IL BmimPF₆.

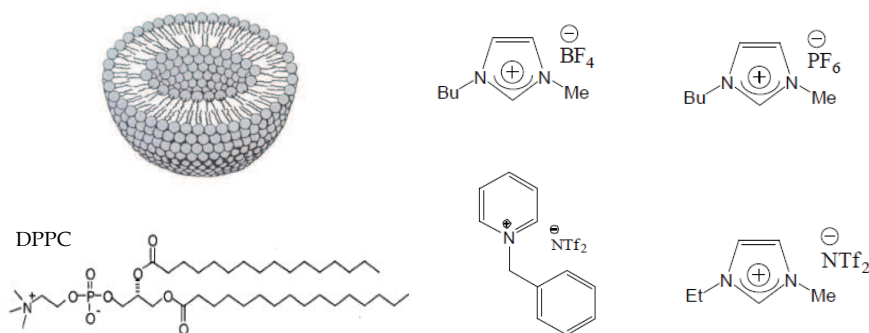


Fig. 5. Chemical structures of ILs and DPPC used to study the formation of vesicles in ILs.

In a more recent study, vesicle structures were obtained with a Zn^{2+} -fluorous surfactant ($[Zn(OOC-CH_2C_6F_{13})_2]$) and a Zn^{2+} -fluorous surfactant/zwitterionic surfactant mixture ($[Zn(OOC-CH_2C_6F_{13})_2]/C_{14}DMAO$) in bmimBF₄ and bmimPF₆ (Hao et al., 2005). The authors determined the size and interlamellar spacing between the bilayers in the vesicles through FF-TEM and SAXS observations. Diameters were about 30 to 90 nm and about 20 to 150 nm in bmimPF₆ for $[Zn(OOC-CH_2C_6F_{13})_2]$ and $[Zn(OOC-CH_2C_6F_{13})_2]/C_{14}DMAO$ respectively. The membrane thickness was about 51.9 Å.

The formation of vesicles from glycerophospholipids (DPPC) was investigated in bmimBF₄, bmimPF₆, emimNTf₂ and bnPyNTf₂ (Figure 5) (Gayet et al., 2010a). Multilamellar vesicles (MLV) were formed using the method of dehydration-rehydration usually employed in water (see section 2.2) (Lasic, 1988). Aggregates formed from DPPC in ILs are first visualized by negative-staining transmission electronic microscopy. As shown in Figure 6a, they are distinctly spherical with diameters of about 200 nm to 1000 nm.

In order to assess vesicle formation, the morphological characteristics of those aggregates in ILs in particular membrane thickness was further investigated by SANS (Figure 6b). Better results were obtained with hydrogenated DPPC in a deuterated IL (bnPyNTf₂D). At low q , the curve is flattening as expected for the typical q^{-2} dependence characteristic of the flat membrane of large vesicles (Chen et al., 1980). Whereas a Bragg peak at $q \sim 0.098 \text{ \AA}^{-1}$ ($d \sim 64 \text{ \AA}$) was observed with water, only a small bump is observed at large q in the case of bnPyNTf₂D. From the latter, we deduced a mean bilayer thickness of $d \sim 63 \pm 1 \text{ \AA}$. Moreover self-assembly of the solutions of DPPC in bnPyNTf₂D could be a mixture of vesicles and small amount of lamellar phase.

The phase physical properties of MLV were further investigated by DSC. As in water, an endothermic pre-transition that corresponds to the transition from the lamellar gel phase ($L_{\beta'}$) to the ripple-gel phase ($P_{\beta'}$), followed by the main transition that corresponds to the

transition to a liquid crystalline phase (L_{α}) were detected in ILs. As shown in Table 3, the values were slightly higher in ILs.

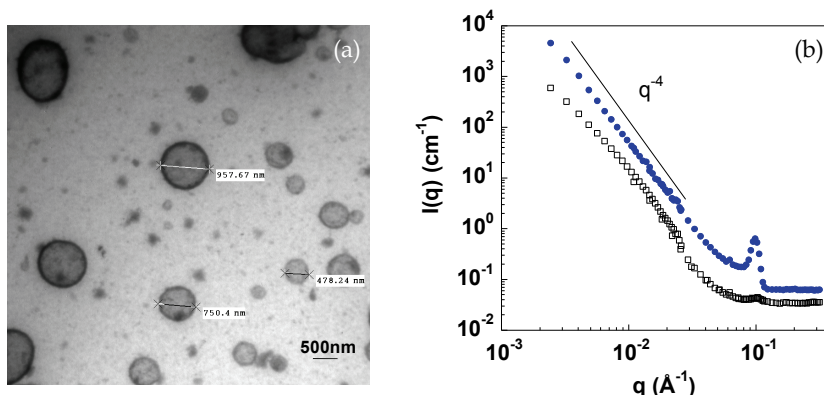


Fig. 6. (a) Negative staining-TEM of vesicles of DPPC in bmimBF_4 . Sodium phosphotungstate was used as the negatively charged dye. (The smallest spots correspond to the IL); (b) SANS curves of DPPC solutions in D_2O (●) and in $\text{bnPyNTf}_2 \text{ D}$ (□); $[\text{DPPC}] = 1 \text{ \%w/v}$ (Gayet et al, 2010).

Solvent	$L_{\beta'} \rightarrow P_{\beta'}$		$P_{\beta'} \rightarrow L_{\alpha}$	
	T (°C)	ΔH (kJ/mol)	T (°C)	ΔH (kJ/mol)
bmimBF_4	55.9	0.5 ± 0.1	61.7	85 ± 2
bmimPF_6	48.5	0.4 ± 0.1	57.5	85 ± 2
emimNTf_2	50.5	7.1 ± 1.8	56.5	92 ± 6
bnPyNTf_2	52.0	0.3 ± 0.2	56.3	89 ± 2
H_2O	36.9	1.6 ± 0.7	44.4	42 ± 2

Table 3. Thermodynamic parameters of the phase transitions of DPPC MLV in bmimBF_4 , bmimPF_6 , bmimNTf_2 , bnPyNTf_2 and in water determined by DSC measurements.

5. Microemulsions

Microemulsions are thermodynamically stable, isotropic and optically transparent dispersions of two immiscible liquids stabilized by a surfactant or by a surfactant/co-surfactant mixture (Zana, 1995). Water-containing microemulsions have been extensively used in separation, drug delivery, nanomaterial synthesis and biocatalysis (Engberts et al., 2006; Holmberg, 2007). As water-in-oil or oil-in-water microemulsions are good solvents for both polar and non-polar substrates, they are also useful for carrying out chemical reactions and usually enhance reactivity and regio/stereoselectivity (Holmberg, 2007).

In the past decade, non aqueous microemulsions, in which water is replaced by polar solvents such as formamide, glycerol, glycol or dimethylformamide, have attracted great interest from both theoretical and practical points of view (Ray and Moulik, 1994). Furthermore, it has been reported that these systems have a number of distinct advantages

over aqueous ones, especially when used as media for organic reactions which need to avoid contact with water (Das et al., 1987). Of special interest is the use in of ionic liquid (IL) microemulsions (Qiu and Texter, 2008). In recent years, ILs have been used as each of the three components required to formulate a microemulsion – the “water like” solvent, the hydrophobic solvent, and/or the surfactant. Recently great attention has been focused on non-aqueous ionic liquid/oil microemulsions. It has been shown that common ILs including 1-butyl-3-imidazolium tetrafluoroborate (bmimBF₄) can be dispersed in certain non-polar organic solvents (cyclohexane, *p*-xylene, benzene and toluene) to form reverse IL-in-oil microemulsions stabilized by non-ionic surfactants. Electron microscopy, light scattering, and small-angle neutron scattering results have provided evidence for the existence of nanodomains of the type IL-in-oil in microemulsions (Gao et al., 2004; Eastoe et al., 2005). They have furthermore shown a regular increase in droplet volume with added IL (Eastoe et al., 2005). BmimPF₆ was also used as a polar solvent in non-aqueous microemulsions and were studied by small-angle X-ray scattering (Li et al., 2005). In spite of the broad spectrum of structural research undertaken in IL microemulsions, their effect on reactivity poses many intriguing questions, the answers to which could open the way to enhancing their potential applications. Reverse IL-in-oil microemulsions may have potential applications owing to the unique features of ILs and of microemulsions: they offer a wide choice of structures (e.g. cation/anion), such as chiral structures, and allow the use of a lower quantity of ionic liquid compared to bulk-phase IL reactions. Moreover these nanostructured surfactant assemblies provide hydrophobic or hydrophilic nanodomains, thereby expanding the potential uses of ILs in reactions. Lastly, changing the microemulsion size could allow one to tune the ratio of unbounded to bounded IL (due to interactions with the polar heads of the surfactants) and hence its solvation properties. This confinement can enable reactivity to be controlled. The formation of non-aqueous microemulsions from a ternary system composed of an ionic liquid (benzylpyridinium bis(trifluoromethanesulfonyl)imide), a nonionic surfactant (polyethylene glycol *p*-(1,1,3,3-tetramethylbutyl)-phenyl ether, TX-100) and toluene was studied (Figure 7) (Gayet et al., 2008).

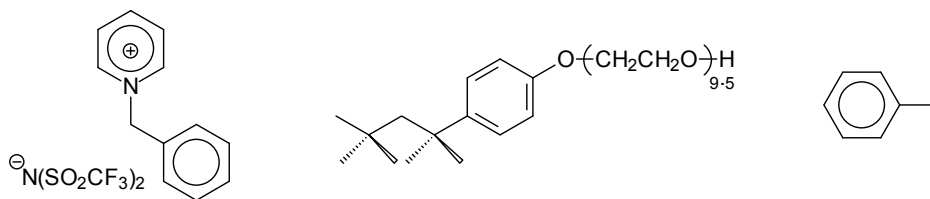


Fig. 7. Chemical structures of IL (benzylpyridinium bis(trifluoromethanesulfonyl) imide, bnPyrNTf₂), surfactant (polyethylene glycol *p*-(1,1,3,3-tetramethylbutyl)-phenyl ether, TX-100) and oil (toluene) used to study the formation of microemulsions.

5.1 Ternary phase diagram

The phase diagram of this ternary system was built by direct observation of the phase behaviour and by conductrimetry at 27°C (Figure 8). Three micro-regions were identified by conductivity measurements according to the percolation theory (Clause et al., 1981).

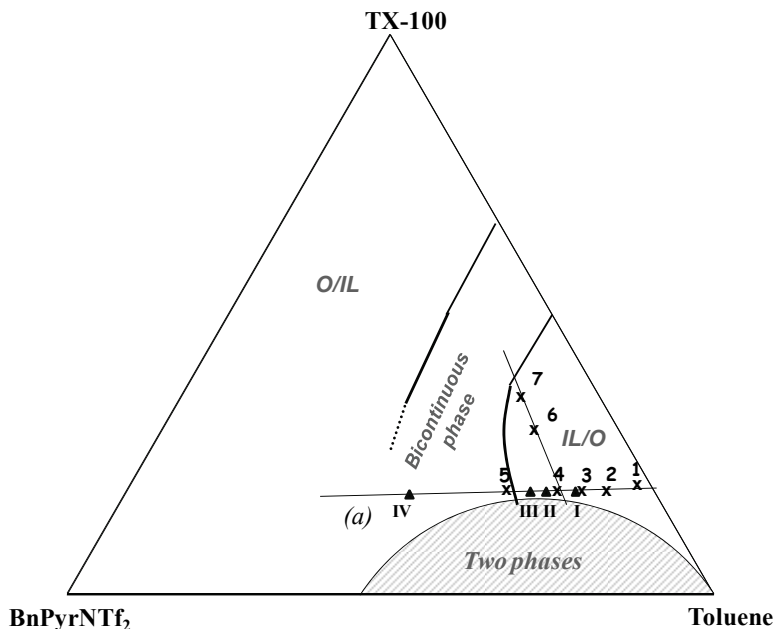


Fig. 8. Phase diagram of BnPyrNTf₂/TX-100/toluene three-component system at 27°C. O/IL, bicontinuous and IL/O are toluene-in-bnPyrNTf₂, bicontinuous phase and bnPyrNTf₂-in-toluene regions respectively (Gayet et al, 2009).

5.2. Structural studies in the microemulsion IL/O region.

PGSE NMR Self-Diffusion and DLS Measurements. The sizes of IL-in-oil microemulsions with various IL fractions were then determined by pulse field gradient spin-echo NMR and by dynamic light scattering measurements. Translational displacements over macroscopic distances were monitored using molecular self-diffusion coefficients (D). Its values are sensitive to friction, obstruction and solvation phenomena, but in particular to confinement in closed domains. They can therefore be used to obtain information on solution microstructure (Fedotov et al., 1996; Yagmur et al., 2003). Figure 9 shows the values of self-diffusion of bnPyrNTf₂, TX-100 and toluene as a function of the total volume fraction of TX-100 and IL along dilution line (a) for samples 2, 3 and 4 in Figure 8. The self-diffusion coefficients of TX-100 and IL are equal and are one order of magnitude less than that of toluene. As the three components have roughly the same size, this implies that the IL and surfactant diffuse together as one entity in toluene.

The hydrodynamic radius R_h of the IL micelles in this toluene phase rich region can be roughly estimated using the Stokes-Einstein equation:

$$R_h = k_B T / (6\pi\eta D) \text{ with } D = D_\infty(1 - k\Phi)$$

where D_∞ is the micelle diffusion coefficient at infinite dilution, k is a constant and Φ is the volume fraction of both TX-100 and IL (Fedotov et al., 1996; Nyden, 2001). R_h values obtained are summarized in Table 4 for both PGSE NMR and DLS measurements. Average sizes thus obtained are compatible with a microemulsion structure.

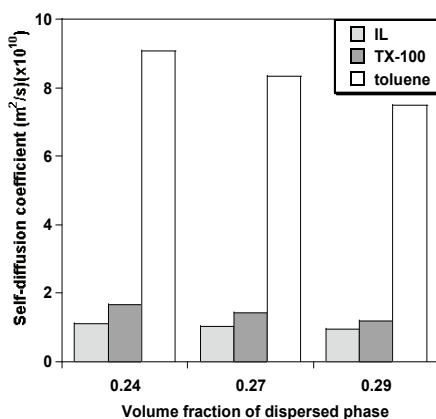


Fig. 9. Self Diffusion coefficients of TX-100, toluene and IL (bnPyrNTf₂) obtained by PGSE NMR plotted as the volume fraction of the droplets i.e. volume fraction of TX-100+IL (standard deviation was below $0.2 \cdot 10^{-10} \text{ m}^2 \cdot \text{s}^{-1}$).

SANS measurements. SANS measurements were employed to determine the structural features of microemulsions and the respective arrangement of IL and TX-100, by using three different contrasts. The first set of SANS data, named “full contrast”, was obtained with microemulsions in deuterated toluene and allowed the determination of the global form of objects. Data obtained with deuterated ionic liquid in hydrogenated toluene and Triton X100 show the objects formed by IL: it is “core contrast” since IL is assumed to be in the core of the micelles. Third, data obtained in toluene mixture, which matches the deuterated ionic liquid, give the scattering from the TX-100 object: it is named “shell contrast”.

Number μE	ϕ_{IL}	$\phi_{\text{TX-100}}$	R_g (nm)	R_g (nm)	R_g (nm)	R_h (nm)	R_h (nm)
			Full contrast (SANS)	Core contrast (SANS)	Shell contrast (SANS)	(PGSE NMR)	(DLS)
1	0.02	0.18	2.00±0.05	2.08±0.05	2.00±0.05	n.d.	n.d.
2	0.06	0.18	2.9±0.1	3.3±0.1	3.1±0.1	1.8±0.2	3.4±0.8
3	0.08	0.19	2.9±0.1	n.d.	2.8±0.1	1.8±0.2	2.4±0.7
4	0.1	0.19	2.8±0.1	2.8±0.1	2.6±0.1	1.9±0.2	2.2±0.8
5	0.15	0.19	1.6±0.1	2.4±0.1	1.5±0.2	n.d.	n.d.
6	0.1	0.27	1.10±0.05	1.13±0.05	0.90±0.05	n.d.	n.d.
7	0.1	0.36	0.72±0.05	0.86±0.05	0.64±0.05	n.d.	n.d.

Table 4. Apparent radii of gyration of bnPyrNTf₂/TX-100/toluene microemulsions deduced from SANS in different contrast conditions^a. ^aHydrodynamic radii deduced from PGSE NMR and DLS measurements. ϕ_{IL} and $\phi_{\text{TX-100}}$ are the volume fractions of bnPyrNTf₂ (the IL) and TX-100 (the surfactant). In μE 1 to 5, $\phi_{\text{TX-100}}$ was kept constant (~0.18-0.19) and ϕ_{IL} increased. In μE 6 and 7, ϕ_{IL} was fixed at 0.1 and $\phi_{\text{TX-100}}$ increased. n.d.: not determined

Typical curves for bnPyNTf₂/TX-100/Toluene mixtures in the microemulsion IL/O region of the phase diagram are shown in Figure 10 for three different contrasts (full contrast, core contrast and shell contrast). Both intensities and shapes look similar: the scattering signals, which are not very strong, decrease with increasing q , while they level off at low q values. Such similar curves indicate that whole objects, the objects formed by IL and those formed by surfactant are not very different.

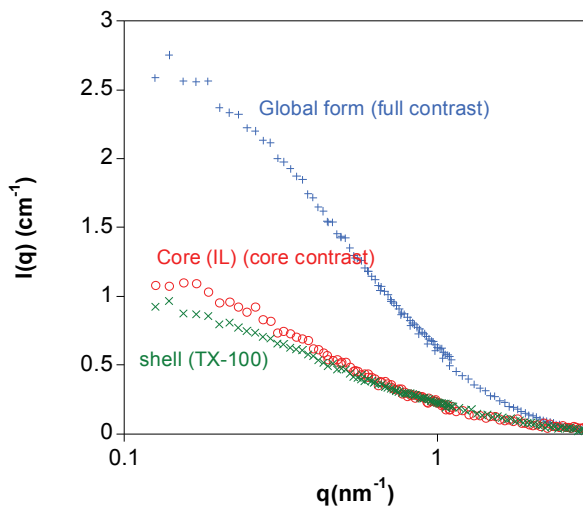


Fig. 10. SANS of bnPyNTf₂/TX-100/Toluene μ E 2 ($\phi_{IL}=0.06$) measured at 27°C in three contrast conditions (+ full contrast, o core contrast, x shell contrast).

These observations were confirmed by the values of the radius of gyration determined from the Guinier plot (around 3 nm, see Table 4). SANS experiments on IL/oil microemulsions clearly demonstrate the formation of surfactant-stabilized dispersed nanodroplets with IL cores.

5.3 Reverse microemulsions as nanoreactors for the Matsuda-Heck reaction

The reverse IL-in-oil microemulsions were used as nanoreactors to perform a Matsuda-Heck reaction between two reactants of opposite polarity, *p*-methoxyphenyl diazonium salt and 2,3-dihydrofuran, in the presence of a palladium catalyst (Figure 11). Two palladium catalysts were used Pd₂(dba)₃·CHCl₃ and a chiral compound bis [(*R*)-1-phenylethylpyridinium] tetrachloropalladate (noted [Pyr]₂[PdCl₄]). This reaction occurred at room temperature and allowed the formation of two regioisomers A and B.

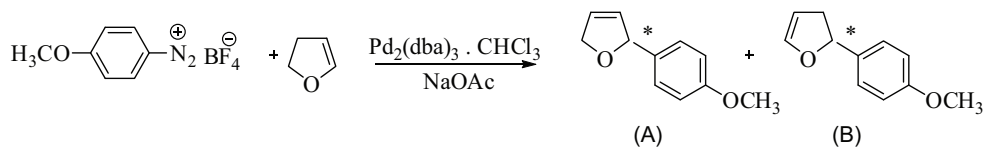


Fig. 11. Matsuda Heck reaction between *p*-methoxyphenyl diazonium salt and 2,3-dihydrofuran using a palladium catalyst.

This reaction was performed at 27°C in pure IL (bnPyrNTf₂), in three IL/O microemulsions (points I, II, and III on line (a) in Figure 8) and in one bicontinuous phase (point IV on line (a) in Figure 8). Only regioisomer A was formed. Yields calculated from GC analysis were up to twice as high in microemulsions (33 to 56%) as those obtained in bulk phase (around 30%) as reported in Table 5. Geometrical constraints and reactant partitioning between the different phases in microemulsions could result in specific orientation of the reactants and catalyst, which have been shown to strongly influence the yield of reaction (Pasc-Banu et al., 2004). Moreover yields became higher on increasing the amount of IL (bicontinuous phase). The use of microemulsions as media for organic reactions suffers from one inherent drawback: the need of large amounts of surfactant to form microemulsions which then have to be separated from the products. However, it is possible, by using a non-ionic surfactant such as here TX-100 to break the single-phase ternary oil-IL-surfactant systems used as reaction media into a 2-phase system by increasing the temperature (called Winsor systems). In the system studied here, an increase in temperature of 27°C to 36°C reversibly changed a Winsor I system (reaction media) into a Winsor II system involving separation of the IL phase and the toluene phase. The products were extracted from the organic phase and the IL phase containing NPs of Pd was successfully reused for another run.

Yields (%) in bnPyrNTf ₂	Yields (%) in microemulsions	
28 ⁱ (33) ⁱⁱ	I	33 ⁱ (37) ⁱⁱ
	II	35 (45)
	III	47 (54)
	IV	51 (56)

Table 5. Yields obtained for Matsuda Heck coupling between the *p*-methoxyphenyl diazonium salt and 2, 3-dihydrofuran using Pd₂(dba)₃·CHCl₃ⁱ or [Pyr]₂[PdCl₄]ⁱⁱ as catalyst (1% mol) in microemulsions I, II, III and IV formed with bnPyrNTf₂ (on line (a) of Figure 8) at 27°C. Standard deviation on yields was around 2%.

The reaction yields obtained greater in microemulsions than in pure IL highlight a strong effect of confinement. Moreover, a direct correlation between the quantity of IL and the reaction yield was observed. IL in oil microemulsions confined the reaction and offered the advantage of using a smaller quantity of ionic liquid compared to bulk phase.

6. Conclusion

In this article, we have discussed the use of ionic liquids as solvent for the self-assembly of surfactants. In ionic liquids, the formation of the same types of amphiphile self-assembly phases as aqueous systems (micelles, vesicles and microemulsions) was evidenced. These aggregates were characterized by surface tension measurements, differential scanning calorimetry, scattering experiments (DLS and SANS), pulse field gradient spin-echo NMR, electrical conductivity measurements, electron microscopy.

Our experiments demonstrated that micelle formation is possible in ILs and that size and aggregation number of the micelles can be tuned by changing the exact nature of the IL. Moreover, as observed in water the formation of lamellar structures of DPPC in different ILs was demonstrated. Lastly three micro-regions of the microemulsion – ionic liquid in oil, bicontinuous and oil in ionic liquid - were identified in the ternary system

bnPyrNTf₂/TX-100/toluene. The reverse IL-in-oil microemulsions have an average gyration radius of approximately 2-3 nm. The reverse IL-in-oil microemulsions were used for the first time as nanoreactors to perform an organic reaction. In addition to the well-known benefits induced by the use of RTILs as solvents, the confinement of IL improved the reactivity of Matsuda-Heck coupling and displayed the advantage of using less ionic liquid than a reaction in the bulk phase. These positive effects can be used in various domains such as biocatalysis or nanomaterials synthesis.

Surfactant self-assembly should open unique opportunities to design nanoscale architectures in green solvents. Such nanostructures are interesting not only from the standpoint of the assembly of advanced materials and environmental concerns, but also may be useful in applications in nanoscience such as nanoreactors for organic and inorganic synthesis, templates for the synthesis of nanostructured materials and in formulation.

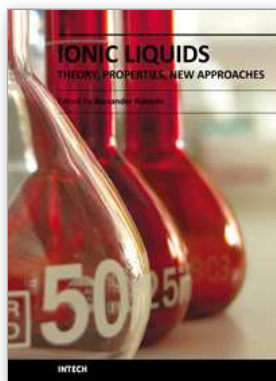
7. References

- Anderson, J. L.; Pino, V.; Hagberg, E. C.; Sheares, V. V. and Armstrong, D. W. (2003). Surfactant solvation effects and micelle formation in ionic liquids. *Chemical Communications*, 2444-2445.
- Araos, M. U. and Warr, G. G. (2005). Self-assembly of nonionic surfactants into lyotropic liquid crystals in ethylammonium nitrate, a room-temperature ionic liquid. *Journal of Physical Chemistry B*, 109, 30, 14275-14277.
- Araos, M. U. and Warr, G. G. (2008). Structure of nonionic surfactant micelles in the ionic liquid ethylammonium nitrate. *Langmuir*, 24, 17, 9354-9360.
- Berthod, A.; Tomer, S. and Dorsey, J. G. (2001). Polyoxyethylene alkyl ether nonionic surfactants: physicochemical properties and use for cholesterol determination in food. *Talanta*, 55, 1, 69-83.
- Chen, S. C.; Sturtevant, J. M. and Gaffney, B. J. (1980). Scanning calorimetric evidence for a 3rd phase-transition in phosphatidylcholine bilayers. *Proceedings of the National Academy of Sciences of the United States of America-Biological Sciences*, 77, 9, 5060-5063.
- Clause, M.; Peyrelasse, J.; Heil, J.; Boned, C. and Lagourette, B. (1981). Bicontinuous structure zones in microemulsions. *Nature*, 293, 5834, 636-638.
- Couper, A.; Gladden, G. P. and Ingram, B. T. (1975). Adsorption of Surface-Active Agents in a Non-Aqueous Solvent. *Faraday Discussions*, 59, 59, 63-75.
- Das, K. P.; Ceglie, A. and Lindman, B. (1987). Microstructure of formamide microemulsions from NMR self-diffusion measurements. *Journal of Physical Chemistry*, 91, 11, 2938-2946.
- Dupont, J.; de Souza, R. F. and Suarez, P. A. Z. (2002). Ionic liquid (molten salt) phase organometallic catalysis. *Chemical Reviews*, 102, 10, 3667-3691.
- Eastoe, J.; Gold, S.; Rogers, S. E.; Paul, A.; Welton, T.; Heenan, R. K. and Grillo, I. (2005). Ionic liquid-in-oil microemulsions. *Journal of the American Chemical Society*, 127, 20, 7302-7303.
- Engberts, J.; Fernandez, E.; Garcia-Rio, L. and Leis, J. R. (2006). Water in oil microemulsions as reaction media for a Diels-Alder reaction between N-ethylmaleimide and cyclopentadiene. *Journal of Organic Chemistry*, 71, 11, 4111-4117.
- Evans, D. F.; Kaler, E. W. and Benton, W. J. (1983). Liquid-crystals in a fused salt-beta, alpha-distearoylphosphatidylcholine in N-ethylammonium nitrate. *Journal of Physical Chemistry*, 87, 4, 533-535.

- Evans, D. F.; Yamauchi, A.; Roman, R. and Casassa, E. Z. (1982). Micelle formation in ethylammonium nitrate, a low-melting fused salt. *Journal of Colloid and Interface Science*, 88, 89-96.
- Fainerman, V. B.; Lucassen-Reynders, E. and Miller, R. (1998). Adsorption of surfactants and proteins at fluid interfaces. *Colloids and Surfaces a-Physicochemical and Engineering Aspects*, 143, 2-3, 141-165.
- Fedotov, V. D.; Zuev, Y. F.; Archipov, V. P.; Idiyatullin, Z. S. and Garti, N. (1996). A Fourier transform pulsed-gradient spin echo nuclear magnetic resonance self-diffusion study of microemulsions and the droplet size determination. 11th International Symposium on Surfactants in Solution, Jerusalem, Israel.
- Fletcher, K. A. and Pandey, S. (2004). Surfactant aggregation within room-temperature ionic liquid 1-ethyl-3-methylimidazolium bis(trifluoromethylsulfonyl)imide. *Langmuir*, 20, 1, 33-36.
- Gao, H. X.; Li, J. C.; Han, B. X.; Chen, W. N.; Zhang, J. L.; Zhang, R. and Yan, D. D. (2004). Microemulsions with ionic liquid polar domains. *Physical Chemistry Chemical Physics*, 6, 11, 2914-2916.
- Gayet, F.; El Kalamouni, C.; Lavedan, P.; Marty, J. D.; Brulet, A. and Lauth-de Viguerie, N. (2009). Ionic Liquid/Oil Microemulsions as Chemical Nanoreactors. *Langmuir*, 25, 17, 9741-9750.
- Gayet, F.; Marty, J.-D. and Lauth-de Viguerie, N. (2008). Palladate Salts from Ionic Liquids as Catalysts in the Heck Reaction. *Arkivoc*, 17, 61-76.
- Gayet, F.; Marty, J. D.; Brulet, A. and Lauth-de Viguerie, N. (2010). Liposomes in ionic liquids. *submitted*.
- Gayet, F.; Marty, J.-D.; Brulet, A. and Lauth-de Viguerie, N. (2011). Vesicles in ionic liquids. *Under press*.
- Gayet, F.; Patrascu, C.; Marty, J. D. and Lauth-de Viguerie, N. (2010). Surfactant Aggregates in Ionic Liquids and Reactivity in Media. *International Journal of Chemical Reactor Engineering*, 8.
- Greaves, T. L. and Drummond, C. J. (2008). Ionic liquids as amphiphile self-assembly media. *Chemical Society Reviews*, 37, 8, 1709-1726.
- Hao, J. and Zemb, T. (2007). Self-assembled structures and chemical reactions in room-temperature ionic liquids. *Current Opinion in Colloid & Interface Science*, 12, 129-137.
- Hao, J. C.; Song, A. X.; Wang, J. Z.; Chen, X.; Zhuang, W. C.; Shi, F.; Zhou, F. and Liu, W. M. (2005). Self-assembled structure in room-temperature ionic liquids. *Chemistry-a European Journal*, 11, 13, 3936-3940.
- Herrington, T. M. and Sahi, S. S. (1988). Temperature-Dependence of the Micellar Aggregation Number of N-Dodecylpolyethyleneoxide Surfactants. *Journal of Colloid and Interface Science*, 121, 1, 107-120.
- Holmberg, K. (2007). Organic reactions in microemulsions. *European Journal of Organic Chemistry*, 5, 731-742.
- Jonstromer, M.; Sjöberg, M. and Warnheim, T. (1990). Aggregation and Solvent Interaction in Nonionic Surfactant Systems with Formamide. *Journal of Physical Chemistry*, 94, 19, 7549-7555.
- Kimizuka, N. and Nakashima, T. (2001). Spontaneous self-assembly of glycolipid bilayer membranes in sugar-philic ionic liquids and formation of ionogels. *Langmuir*, 17, 22, 6759-6761.

- Lasic, D. D. (1988). The mechanism of vesicle formation. *Biochemical Journal*, 256, 1, 1-11.
- Li, J. C.; Zhang, J. L.; Gao, H. X.; Han, B. X. and Gao, L. (2005). Nonaqueous microemulsion-containing ionic liquid [bmim][PF₆] as polar microenvironment. *Colloid and Polymer Science*, 283, 12, 1371-1375.
- McDonald, C. (1967). Micellar Properties of Some Non-Ionic Surface-Active Agents in Polar Solvents. *Journal of Pharmacy and Pharmacology*, 19, 6, 411-&.
- Merrigan, T. L.; Bates, E. D.; Dorman, S. C. and Davis, J. H. (2000). New fluoros ionic liquids function as surfactants in conventional room-temperature ionic liquids. *Chemical Communications*, 20, 2051-2052.
- Nakashima, T. and Kimizuka, N. (2002). Vesicles in salt: Formation of bilayer membranes from dialkyldimethylammonium bromides in ether-containing ionic liquids. *Chemistry Letters*, 10, 1018-1019.
- Nyden, M. (2001). *Handbook of Applied Surface and Colloid Chemistry*, John Wiley and sons, Ltd.
- Pasc-Banu, A.; Sugisaki, C.; Gharsa, T.; Marty, J. D.; Gascon, I.; Pozzi, G.; Quici, S.; Rico-Lattes, I. and Mingotaud, C. (2004). A catalytic Langmuir film as a model for heterogeneous and homogeneous catalytic processes. *Angewandte Chemie-International Edition*, 43, 45, 6174-6177.
- Patrascu, C.; Gauffre, F.; Nallet, F.; Bordes, R.; Oberdisse, J.; de Lauth-Viguerie, N. and Mingotaud, C. (2006). Micelles in ionic liquids: Aggregation behavior of alkyl poly(ethyleneglycol)-ethers in 1-butyl-3-methyl-imidazolium type ionic liquids. *Chemphyschem*, 7, 1, 99-101.
- Patrascu, C.; Sugisaki, C.; Mingotaud, C.; Marty, J. D.; Genisson, Y. and Lauth-de Viguerie, N. (2004). New pyridinium chiral ionic liquids. *Heterocycles*, 63, 9, 2033-2041.
- Qiu, Z. and Texter, J. (2008). Ionic liquids in microemulsion. *Current Opinion in Colloid & Interface Science*, 13, 252-262.
- Ranke, J.; Stolte, S.; Stormann, R.; Arning, J. and Jastorff, B. (2007). Design of sustainable chemical products - The example of ionic liquids. *Chemical Reviews*, 107, 6, 2183-2206.
- Ray, S. and Moulik, S. P. (1994). Dynamics and thermodynamics of aerosol-OT-aided nonaqueous microemulsions. *Langmuir*, 10, 8, 2511-2515.
- Rosen, M. J.; Cohen, A. W.; Dahanayake, M. and Hua, X. Y. (1982). Relationship of Structure to Properties in Surfactants .10. Surface and Thermodynamic Properties of "2-Dodecyloxypoly(Ethenoxyethanol)S, C₁₂H₂₅(O₂C₂H₄)Xoh, in Aqueous-Solution. *Journal of Physical Chemistry*, 86, 4, 541-545.
- Tran, C. D. and Yu, S. F. (2005). Near-infrared spectroscopic method for the sensitive and direct determination of aggregations of surfactants in various media. *Journal of Colloid and Interface Science*, 283, 2, 613-618.
- van Os, N. M.; Haas, S. S. and Rupert, L. A. M. (1993). Physico-Chemical properties of selected anionic, cationic and nonionic surfactants. New-York.
- Wang, L. Y.; Chen, X.; Chai, Y. C.; Hao, J. C.; Sui, Z. M.; Zhuang, W. C. and Sun, Z. W. (2004). Lyotropic liquid crystalline phases formed in an ionic liquid. *Chemical Communications*, 24, 2840-2841.
- Yaghmur, A.; Aserin, A.; Antalek, B. and Garti, N. (2003). Microstructure considerations of new five-component Winsor IV food-grade microemulsions studied by pulsed gradient spin-echo NMR, conductivity, and viscosity. *Langmuir*, 19, 4, 1063-1068.

- Zana, R. (1995). Aqueous surfactant-alcohol systems: a review. *Advances in Colloid and Interface Science*, 57, 1-64.
- Zulauf, M.; Weckstrom, K.; Hayter, J. B.; Degiorgio, V. and Corti, M. (1985). Neutron-scattering study of micelle structure in isotropic aqueous-solutions of poly(oxyethylene) amphiphiles. *Journal of Physical Chemistry*, 89, 15, 3411-3417.



Ionic Liquids: Theory, Properties, New Approaches

Edited by Prof. Alexander Kokorin

ISBN 978-953-307-349-1

Hard cover, 738 pages

Publisher InTech

Published online 28, February, 2011

Published in print edition February, 2011

Ionic Liquids (ILs) are one of the most interesting and rapidly developing areas of modern physical chemistry, technologies and engineering. This book, consisting of 29 chapters gathered in 4 sections, reviews in detail and compiles information about some important physical-chemical properties of ILs and new practical approaches. This is the first book of a series of forthcoming publications on this field by this publisher. The first volume covers some aspects of synthesis, isolation, production, modification, the analysis methods and modeling to reveal the structures and properties of some room temperature ILs, as well as their new possible applications. The book will be of help to chemists, physicists, biologists, technologists and other experts in a variety of disciplines, both academic and industrial, as well as to students and PhD students. It may help to promote the progress in ILs development also.

How to reference

In order to correctly reference this scholarly work, feel free to copy and paste the following:

J. D. Marty and N. Lauth de Viguerie (2011). Aggregates in Ionic Liquids and Applications Thereof, Ionic Liquids: Theory, Properties, New Approaches, Prof. Alexander Kokorin (Ed.), ISBN: 978-953-307-349-1, InTech, Available from: <http://www.intechopen.com/books/ionic-liquids-theory-properties-new-approaches/aggregates-in-ionic-liquids-and-applications-thereof>

INTECH

open science | open minds

InTech Europe

University Campus STeP Ri
Slavka Krautzeka 83/A
51000 Rijeka, Croatia
Phone: +385 (51) 770 447
Fax: +385 (51) 686 166
www.intechopen.com

InTech China

Unit 405, Office Block, Hotel Equatorial Shanghai
No.65, Yan An Road (West), Shanghai, 200040, China
中国上海市延安西路65号上海国际贵都大饭店办公楼405单元
Phone: +86-21-62489820
Fax: +86-21-62489821

© 2011 The Author(s). Licensee IntechOpen. This chapter is distributed under the terms of the [Creative Commons Attribution-NonCommercial-ShareAlike-3.0 License](#), which permits use, distribution and reproduction for non-commercial purposes, provided the original is properly cited and derivative works building on this content are distributed under the same license.